Molecular and Cellular Pathobiology

Cancer Research

Endocrine Fibroblast Growth Factor FGF19 Promotes Prostate Cancer Progression

Shu Feng[1], Olga Dakhova[1], Chad J. Creighton[2], and Michael Ittmann[1]

Abstract

Prostate cancer is the most common visceral malignancy and the second leading cause of cancer deaths in US men. There is broad evidence that fibroblast growth factor (FGF) receptors are important in prostate cancer initiation and progression, but the contribution of particular FGFs in this disease is not fully understood. The FGF family members FGF19, FGF21, and FGF23 comprise a distinct subfamily that circulate in serum and act in an endocrine manner. These endocrine FGFs require α-Klotho (KL) and/or β-Klotho (KLB), two related single-pass transmembrane proteins restricted in their tissue distribution, to act as coreceptors along with classic FGF receptors (FGFR) to mediate potent biologic activity. Here we show that FGF19 is expressed in primary and metastatic prostate cancer tissues, where it functions as an autocrine growth factor. Exogenous FGF19 promoted the growth, invasion, adhesion, and colony formation of prostate cancer cells at low ligand concentrations. FGF19 silencing in prostate cancer cells expressing autocrine FGF19 decreased invasion and proliferation *in vitro* and tumor growth *in vivo*. Consistent with these observations, KL and/or KLB were expressed in prostate cancer cells *in vitro* and *in vivo*, raising the possibility that additional endocrine FGFs may also exert biologic effects in prostate cancer. Our findings support the concept that therapies targeting FGFR signaling may have efficacy in prostate cancer and highlight FGF19 as a relevant endocrine FGF in this setting. *Cancer Res; 73(8); 2551–62. ©2013 AACR.*

Introduction

Prostate cancer is the most common malignancy in American men, affecting 1 in 9 men over 65 years of age. Currently, there is no effective cure for advanced stages of prostate cancer and it is the second-leading cause of male cancer mortality. Identification of novel endogenous factors responsible for proliferation, migration, and invasion of prostate cancer will facilitate the understanding of the biology of prostate cancer progression and the development of new approaches for the diagnosis and treatment of this disease.

The human fibroblast growth factor (FGF) family is composed of 22 structurally related polypeptides. The FGF genes can be divided into 3 major groups (see ref. 1 for review). FGF1-10, 16–18, 20 and 22 are classical FGFs. They are mitogens that bind strongly to heparin, which is abundant in the extracellular microenvironment, so these FGFs tend to act locally. FGFs 11 to 14 are not secreted mitogens and they appear to modulate electrical excitability and as such do not appear to play a role in cancer. A major new discovery in the last decade is the characterization of the endocrine FGFs (FGF15/19, FGF21, and FGF23). FGF15 is the mouse homolog of human FGF19 and has analogous functions in mice. This subfamily is secreted into serum and they are stable in this environment, which allows them to act in an endocrine fashion (2). Another common feature shared by this atypical FGF family is their requirement for α-Klotho (KL) and/or β-Klotho (KLB), 2 related single-pass transmembrane proteins with a restricted tissue distribution for potent biologic activity (3). Both KL and KLB act as coreceptors with the classic FGF receptors (FGFR) in relevant target tissues to facilitate the FGF–FGFR interaction for endocrine FGFs. The tissue-specific actions of the endocrine FGFs are thus modulated by the presence of their specific coreceptors since one or more FGFRs are expressed in most cells. Endocrine FGF subfamily members regulate diverse physiologic processes, namely, energy metabolism and bile acid homeostasis (FGF19; refs. 4–5), glucose and lipid metabolism (FGF21; ref. 6), and phosphate and vitamin D homeostasis (FGF23; ref. 7).

The only endocrine FGF that has been examined in cancer is FGF19. Before the identification of the KL/KLB binding partners for this subfamily, it was reported that FGF19 displays binding specificity for FGFR4 at relatively high concentrations (2, 8); however, studies in HEK293 and L6 cells show that in the presence of KLB, FGF19 binds and signals through multiple FGFRs (9), with FGFR1 and FGFR4 being more potent than FGFR2 or FGFR3. KL can also act as a coreceptor for FGF19

Authors' Affiliations: [1]Department of Pathology and Immunology and Michael E. DeBakey Department of Veterans Affairs Medical Center; and [2]Dan L. Duncan Cancer Center Division of Biostatistics, Baylor College of Medicine, Houston, Texas

Note: Supplementary data for this article are available at Cancer Research Online (http://cancerres.aacrjournals.org/).

Corresponding Author: Michael Ittmann, Department of Pathology and Immunology and Michael E. DeBakey Department of Veterans Affairs Medical Center, Baylor College of Medicine, One Baylor Plaza, Houston, TX 77030. Phone: 713-798-6196; Fax: 713-798-5838; E-mail: mittmann@bcm.tmc.edu

doi: 10.1158/0008-5472.CAN-12-4108

(10–11), although the exact FGFR specificity has not been determined. Although FGF19 was first reported to be expressed in a colon adenocarcinoma cell line a decade ago (8), its relevance to cancer had not been evident until it was discovered that the transgenic mice overexpressing FGF19 in skeletal muscle develop hepatocellular carcinoma (12), which presumably reflects an endocrine action of the increased levels of circulating FGF19. FGF19 has been found to be coexpressed in a subgroup of primary human liver, colonic and lung squamous carcinomas and in a subset of human colon cancer cell lines (13). An anti-FGF19 monoclonal antibody that selectively blocks the interaction of FGF19 with FGFR4 inhibits growth of colon tumor xenografts *in vivo* and effectively prevents hepatocellular carcinomas in FGF19 transgenic mice. The efficacy of the antibody in these models is linked to the inhibition of FGF19-dependent activation of FGFR4 and downstream targets FRS2, ERK, and β-catenin (14). The inactivation of FGF19 could be beneficial for the treatment of malignancies involving the interaction of FGF19 and FGFRs.

All FGF ligands, including endocrine FGFs, signal through 4 highly conserved transmembrane tyrosine kinase receptors (FGFR1–4) with differential affinity for various FGF ligands. FGFR signaling has been strongly implicated in prostate tumorigenesis (15). Our laboratory has shown that FGFR1 is expressed in clinically localized prostate cancers based on immunohistochemistry (IHC) and Western blot analysis of prostate cancer extracts (16). Studies in transgenic mice have shown that chronic FGFR1 activation can lead to adenocarcinoma and epithelial–mesenchymal transition of the cancer cells (17). We (18) and others (19–21) have shown that there is increased expression of FGFR4 in prostate cancer by IHC and this has been confirmed by quantitative RT-PCR (qRT-PCR). Strong FGFR4 expression is significantly associated with poor clinical outcome (19, 21). For example, recent work by Murphy and colleagues (21) has shown that increased FGFR4 expression is strongly associated with prostate cancer-specific death as compared with decreased expression of the FGFR signaling inhibitor Sef. Thus both correlative studies in human tissues and mouse models strongly support the concept that FGFR1 and FGFR4 both play an important role in prostate cancer.

Our group has previously shown that FGF19 is expressed as a paracrine factor in prostate cancer reactive stroma based on analysis of laser-captured normal and prostate cancer stroma (22). However, to date, the role of FGF19 in prostate cancer has not been comprehensively addressed. Our data indicates that FGF19 is expressed in prostate cancer and that FGF19 signaling plays an important role in prostate cancer tumorigenesis and progression.

Materials and Methods

Cell culture

Human prostate cancer cells PC3, LNCaP, DU145, and VCaP and the immortalized normal prostate PNT1a cells were maintained in RPMI-1640 medium (Invitrogen), supplemented with 10% FBS (Invitrogen) and 1% penicillin/streptomycin. Cell lines were authenticated by STR analysis at MD Anderson Cancer Center Characterized Cell Line Core Facility (Houston, TX).

Prostate and prostate cancer tissues

Tissue samples were obtained from Baylor Prostate Cancer Program Tissue Bank and were collected from fresh radical prostatectomy specimens after obtaining informed consent under an Institutional Review Board-approved protocol. Laser capture of epithelial and stromal RNAs from frozen tissues was carried out as described previously (22). Paraffin-embedded tissues from these specimens were used to construct small tissue microarrays for immunohistochemistry.

Transfection

Two human GIPZ lentiviral shRNAmir individual clones (V2LHS_50187 and V2LHS_50189) targeting FGF19 and the GIPZ vector clone obtained from Open Biosystems were transiently transfected into PC3 and DU145 cells with FuGene 6 transfection reagent (Roche) in triplicate in 6-well plates according to manufacturer's instructions. Stable FGF19 knockdown cell lines were generated by infecting PC3 cells with the 2 FGF19 GIPZ lentiviral shRNAmir types and selecting with 1 μg/mL puromycin in growth medium. GIPZ vector was used to produce the vector control PC3 cells.

Cell proliferation assays

To examine the effect of exogenous FGF19, cells were incubated with different concentrations of recombinant FGF19 (R&D Systems) for 48 or 72 hours in serum-free medium. The effect of FGF19 knockdown on PC3 and DU145 cell proliferation was assessed using FGF19 shRNA transient transfection. In brief, DU145 and PC3 cells were plated in 96-well plates, transfected with FGF19 shRNAs, and 48 hours later cell proliferation was measured. Viable cell number was determined using the CellTiter 96 Aqueous One Solution Cell Proliferation Assay (Promega) as described by the manufacturer. Cell viability at 72 hours was assessed by counting viable and nonviable cells based on Trypan blue staining. For stable PC3 FGF19 knockdown cells, cell proliferation was determined using a Coulter counter.

Soft agar colony formation assay

Cell suspensions of 5,000 cells/mL were prepared in 0.35% agar diluted in growth medium and plated on a 0.6% agar foundation in 6-well culture plates with different doses of FGF19, 50 ng/mL FGF2 or vehicle only, and 20 U/mL heparin at 37°C. After culture for 14 days, the cells were stained with 2 mg/mL of p-iodonitrotetrazolium violet (Sigma) and colonies were counted with a dissecting microscope.

Cell adhesion assays

Cells were grown in 6-well plates to 80% confluence, starved with serum-free RPMI-1640 for 24 hours, and then incubated with a variety of concentrations of FGF19 or vehicle in serum-free medium in the presence of 20 U/mL heparin at 37°C for 48 hours. The cells were then detached with 0.25% trypsin-EDTA, washed with PBS twice, resuspended in serum-free medium with 0.5% bovine serum albumin, counted and seeded with a density of 6×10^4 per well into 96-well plates

precoated with 10 ng/mL type I collagen (Sigma) or 1:200 diluted Matrigel (R&D Systems) followed by preblocking with 1% bovine serum albumin. After incubation at 37°C for 1 hour, unbound cells were washed away and the number of cells was quantitated with CellTiter 96 Aqueous One Solution Cell Proliferation Assay.

Matrigel invasion assays

To evaluate the effect of FGF19 on cell invasion, we conducted invasion assays using BD BioCoat Matrigel invasion chambers (Becton Dickinson). After incubation with 25 ng/mL of FGF19 or vehicle only and 20 U/mL of heparin for 24 hours (PC3), 36 hours (DU145), or 72 hours (LNCaP and PNT1a), noninvading cells in the top chambers were removed and the invading cells on the bottom surface of the membrane were fixed and stained with Diff–Quik stain. The membranes were mounted on slides, scanned, and photographed, and all cells were counted.

Xenograft tumors

Male nude mice were injected over each flank with either PC3 with FGF19 knockdown or vector controls cell (2×10^6 cells/site). Tumor volume was measured twice weekly using calipers. All procedures were carried out in accordance with the Institutional Animal Care and Use Committees approved protocol.

RT-PCR and quantitative RT-PCR

To examine expression of FGF19, KL, KLB, or FGFR4 mRNA in human prostate cancer cell lines and/or patient prostate cancer and benign prostate samples, we carried out RT-PCR or quantitative real-time RT-PCR (qRT-PCR). Total RNA was extracted from cell lines using the RNeasy Kit (Qiagen). cDNA was synthesized using an iScript cDNA Synthesis Kit (Bio-Rad) with a blend of Oligo(dT) and random hexamer primers. qRT-PCR was conducted according to a qPCR SybrGreen real-time protocol on the IQ5 iCycler. Primer sequences and PCR conditions are summarized in Supplementary Table S1. All data were normalized to hypoxanthine phosphoribosyltransferase (HPRT) expression. Each measurement point was repeated at least in triplicate for 3 samples and the average and standard deviation were calculated. HPRT was used as a control mRNA.

Western blot

Total cellular protein lysate was prepared as described previously (23). Briefly, cells were lysed in modified RIPA buffer containing Tris 50 mmol/L, NaCl 150 mmol/L, Triton X-100 1%, SDS 0.1%, deoxycholate 0.5%, sodium orthovanadate 2 mmol/L, sodium pyrophosphate 1 mmol/L, NaF 50 mmol/L, EDTA 5 mmol/L, PMSF 1 mmol/L, and 1× protease inhibitor cocktail (Roche) and clarified by centrifugation. Protein concentration of the lysates was determined using the BCA protein assay Kit (Thermo Scientific). Forty micrograms of the extracted protein from each sample was subjected to electrophoresis in 10% to 15% SDS PAGE, dependent on the molecular weight of the proteins to be analyzed. Proteins in the gels were transferred onto Immobilon-P polyvinylidene difluoride membranes (Invitrogen) and subjected to Western blot analysis with different antibodies. The antibodies were from Cell Signaling Technology Inc. and included: phospho-FRS2 (Tyr196) rabbit polyclonal antibody; phospho-p44/42 MAPK (p-Erk1/2) rabbit mAb; p44/42 MAPK (Erk1/2); phospho-p38 MAPK (Thr180/Tyr182) rabbit mAb; phospho-MEK1/2 (Ser217/221) rabbit mAb; MEK1/2 rabbit mAb; phospho-AKT (Ser473) rabbit mAb; phospho-AKT (Thr308) rabbit mAb; and total AKT rabbit mAb. All were used at a 1:1,000 dilution. A goat polyclonal anti-β-actin antibody (Santa Cruz Biotech) was utilized at 1:1,000 as loading control. After incubation with primary antibodies for overnight at 4°C or for 1 hour at room temperature, horseradish peroxidase–labeled secondary antibodies were then applied to the membranes for 1 hour at room temperature. Signals were visualized using enhanced chemiluminescence Western blot analysis detection reagents (Thermo).

Immunohistochemistry

FGF19 IHC was carried out using the general procedures described previously (24). Antigen retrieval was carried out in Tris-EDTA, pH 9.0 for 20 minutes in steamer followed by 20 minutes cooling at room temperature. Anti-FGF19 antibody (R&D Systems, mouse monoclonal, catalog number MAB969) was incubated with sections at a 1:1,200 dilution at 4°C overnight. Detection was carried out at room temperature using a PolyVue Polymer detection system (Diagnostic BioSystems) according to manufacturer's directions. The positive control was paraffin-embedded DU145 cells and the negative control was PNT1a cells. An additional negative control included incubation of prostate tissues with no primary antibody. Immunohistochemistry for KL was conducted as for FGF19 except primary antibody (Calbiochem, rabbit polyclonal, catalog number 423500) that was incubated at 1:100 overnight at 4°C. Positive control was normal kidney. Negative control was carried out with no primary antibody for both kidney and prostate tissue.

FGF19 ELISA

FGF19 expression in stable shRNA-mediated FGF19 gene knockdown PC3 cells was quantified by ELISA. Cell lysates were prepared as described above for Western blot. Protein concentration were determined using the BCA Protein Assay Kit (Thermo) and equal amounts of protein lysates were subjected to ELISA for FGF19 (R&D Systems, catalog number DF1900) as per the manufacturer's instructions.

Gene expression analysis

KL mRNA levels were examined in various public expression datasets, including the "Expo" dataset (GEO accession number GSE2109), of cancers from various histologic subtypes, and the Roth and colleagues (25) dataset, of various normal tissues (GSE3526), as well as 4 different prostate cancer versus benign tissue datasets, via Oncomine (26).

Statistical analysis

Numerical values were compared using the t test or the Mann–Whitney test as appropriate. Differences were considered significant if $P < 0.05$.

Results

Expression of FGF19 in human prostate cancer cell lines

We analyzed FGF19 expression in the commonly used prostate cancer cell lines PC3, LNCaP, DU145, and VCaP, as well as an immortalized normal prostate epithelial cell line PNT1a. qRT-PCR indicates that FGF19 mRNA is expressed in DU145, PC3, and VCaP cells, whereas it is undetectable in LNCaP and PNT1a cells (Fig. 1A). Thus, in 3 of 4 prostate cancer cell lines, there is upregulation of FGF19 signaling relative to the PNT1a immortalized normal epithelial cells.

Expression of Klotho coreceptors in human prostate cancer cell lines

The *KL* gene is expressed in all 5 cell lines tested including normal PNT1a cells, although at the lowest level in PC3 cells. *KLB* is expressed in DU145 and VCaP cells, but it is not detected in PC3, LNCaP, and PNT1a cells by RT-PCR (Fig. 1B). Thus 2 of the 4 prostate cancer cell lines express *KLB*, which is not expressed in the normal prostatic epithelial cell line, whereas *KL* is ubiquitously expressed in both normal and neoplastic prostatic epithelial cells lines.

Effect of FGF19 on prostate cancer cells *in vitro*

Given that Klotho coreceptors are expressed on prostate and prostate cancer cell lines, we sought to determine the effects of exogenous FGF19 on these cells *in vitro*. To evaluate the effect of exogenous FGF19 on prostate cancer cell proliferation *in vitro*, we stimulated PC3, LNCaP, and DU145 prostate cancer cells and PNT1a immortalized normal prostatic epithelial cells with a variety of concentrations of recombinant FGF19 for 48 or 72 hours in serum-free medium and determined the extent of cellular proliferation relative to cells not treated with FGF19. Exogenous FGF19 stimulation enhanced prostate cancer cell proliferation even at doses as low as 0.25 ng/mL (DU145 and LNCaP cells), which is near the mean human physiologic serum FGF19 concentration (27–28; Fig. 2A). FGF19-induced proliferation was lower, but still statistically significant, in PNT1a cells at 10 ng/mL. It is unclear why the PNT1a cells are less sensitive to FGF19-induced proliferation but it might indicate that PNT1a express a negative regulator of FGF19-induced proliferation that is decreased or lost in prostate cancer cell lines.

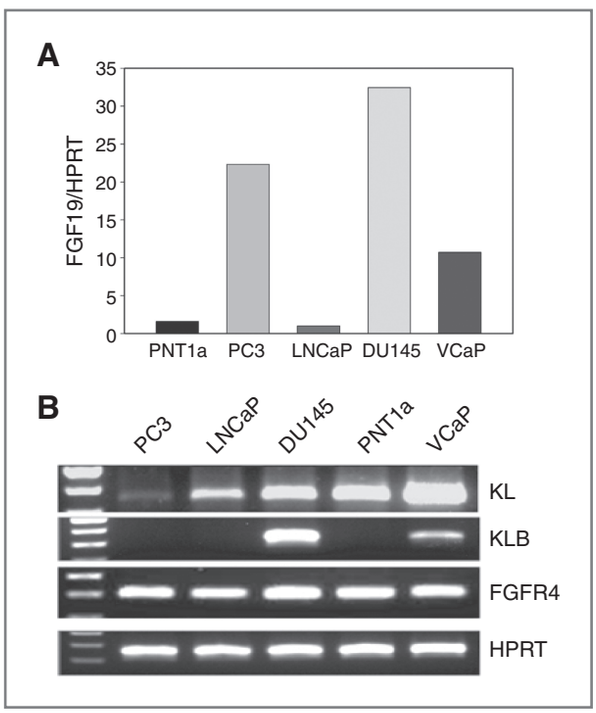

Figure 1. FGF19 and Klotho coreceptors are expressed in prostate and prostate cancer cell lines. A, FGF19 expression was determined by qRT-PCR using RNAs from the indicated cell lines. PNT1a and LNCaP were below the reliable detection limit of this assay. B, expression of KL, KLB, and FGFR4 in PNT1a and prostate cancer cell lines by RT-PCR. HPRT is control for reverse transcription.

FGF19 promotes anchorage independent growth

PC3 and LNCaP cell lines were plated with different concentrations of FGF19 in soft agar and colony formation quantified after 14 days. As shown in Fig. 2B, cells treated with FGF19 formed more colonies in soft agar than vehicle controls and colony numbers were similar to those seen in FGF2-treated cells, indicating that FGF19 promotes anchorage-independent growth capacity *in vitro*.

FGF19 stimulates prostate cancer cell adhesion

The migration of cancer cells is critically regulated by physical adhesion of cells to the extracellular matrix, which is one of the early steps in tumor dissemination (29). Therefore, we investigated whether FGF19 stimulates prostate cancer cell adhesion to the extracellular matrix component type I collagen (COLI) or Matrigel. Cells were preincubated with a variety of concentrations of FGF19 for 48 hours and then subjected to adhesion assay in 96-well plates precoated with COLI or 1:200 dilution of Matrigel. As seen in Fig. 2C, FGF19 significantly enhances PC3 and DU145 cells adhesion on both type I collagen and Matrigel even at concentrations as low as 0.25 ng/mL and 0.5 ng/mL.

FGF19 stimulates prostate cancer cell invasion

To evaluate the effect of FGF19 on prostate cancer cell invasion, we conducted invasion assays using Matrigel invasion chambers. After incubation with or without 25 ng/mL of FGF19 for 24 hours (PC3), 36 hours (DU145), or 72 hours (LNCaP and PNT1a), cell invasion was analyzed as described previously (23). FGF19 promotes prostate cancer cell invasion by approximately 140% to 170% for all cell lines (Fig. 2D).

FGF19 stimulation activates MAP kinase and AKT pathways in prostate cancer cells

To examine the activation of FGFR signaling and its downstream pathways by FGF19, we analyzed phosphorylation of FRS2, p42/44 MAPK (ERK1/2), and p38 MAPK, as well as MEK1/2, by Western blot analysis in DU145 cells after stimulation with FGF19 for 15 minutes. As shown in Fig. 3A, FGF19 actives ERK and p38 MAPK signaling. We then examined the

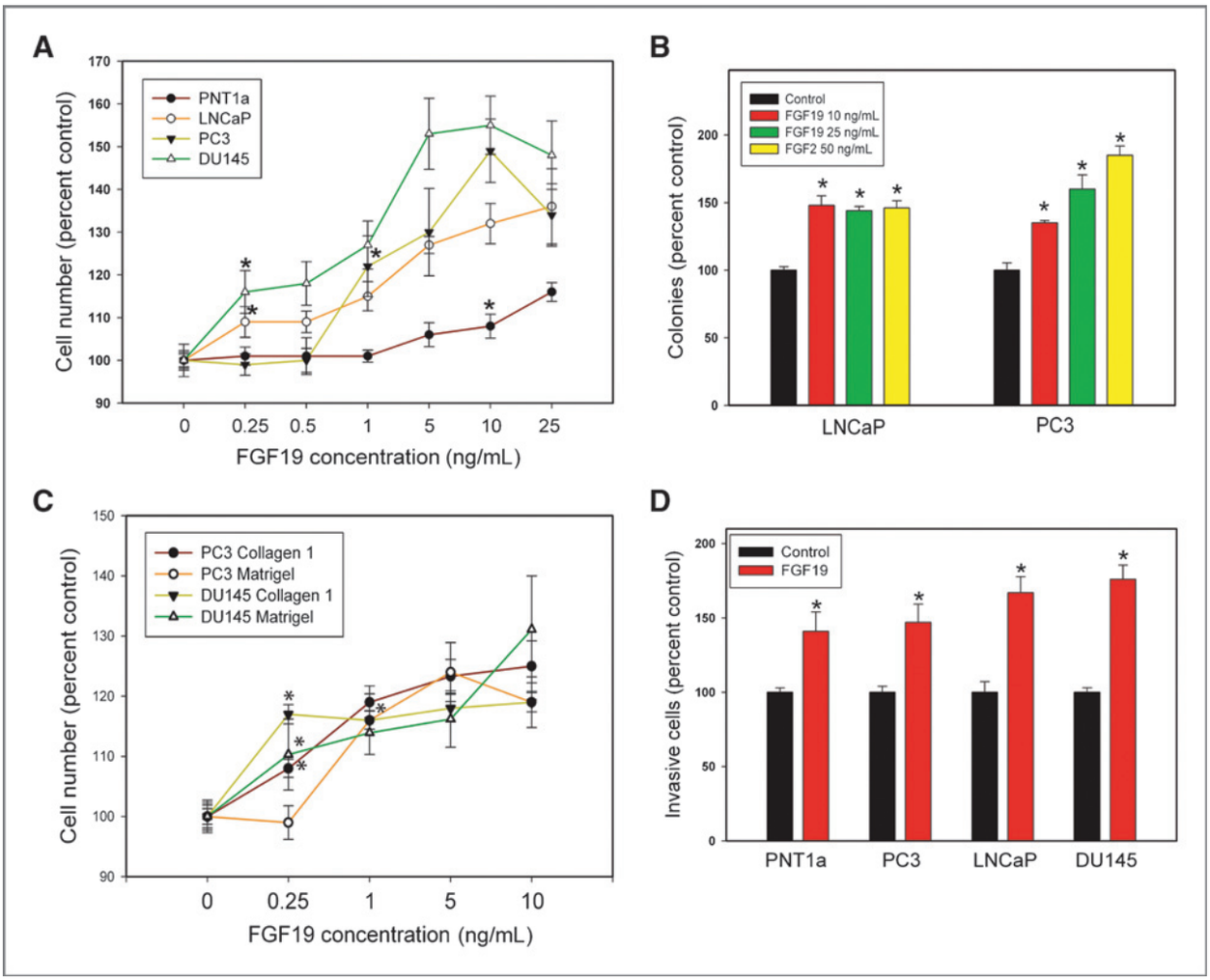

Figure 2. Biologic effects of exogenous FGF19 on prostate and prostate cancer cell lines. A, FGF19-induced proliferation. FGF19 was added to cultures of cells in serum free-medium at the indicated concentration and cell number analyzed at either 48 or 72 hours depending on the cell line. B, colony formation in soft agar. FGF19, FGF2, or vehicle was added to cells in soft agar at the indicated concentration and colonies counted after 14 days. C, FGF19-induced cell adhesion. Numbers of cells adherent to collagen 1 or Matrigel were determined at the indicated FGF19 concentration as described in Materials and Methods. D, invasion through Matrigel. Cell invasion though Matrigel was determined as described in Materials and Methods. Data are expressed relative to vehicle only control (100%). Mean ± SEM for triplicates are shown for all experiments. Asterisks indicate statistically significant differences. For A and C, the first statistically significant concentration for each cell line relative to control is indicated by an asterisk and all differences at higher concentrations are significant but asterisks are omitted for clarity.

activation of the AKT pathway in LNCaP cells, which have inactivation of PTEN, by FGF19. Stimulation of LNCaP cells with FGF19 enhanced AKT activation as evidenced by increased phosphorylation on both S473 and T308 of AKT after 24 or 42 hours (Fig. 3B). The activation of AKT was relatively slow and thus may be an indirect effect of FGF19 stimulation.

FGF19 suppression with shRNA inhibits prostate cancer cell invasion *in vitro* and tumorigenesis *in vivo*

To determine the biologic importance of the autocrine FGF19 produced by the prostate cancer cell lines, we carried out knockdown experiments targeting FGF19. We screened 2 FGF19 GIPZ lentiviral shRNAmir clones (Open Biosystem) for FGF19 knockdown by transient transfection into DU145 and PC3 cells. FGF19 mRNA expression was evaluated by qRT-PCR 48 hours after transfection. Parallel sets of cells were subjected to invasion and proliferation assays. FGF19mRNA expression in DU145 cells was suppressed by 40% to 45% and DU145 invasiveness was inhibited by about 25% to 30% (Fig. 4A). PC3 FGF19 mRNA was decreased by 25% to 50% and invasion was decreased by 45% to 60% (Fig. 4B). The effects on viable cell number were less striking (<10% decrease), although still statistically significant. Of note, there was an associated decrease in cell viability from approximately 96% to 85%–89% for both cell lines using either shRNA (Supplementary Fig. S1). We did not see a statistically significant decrease in Ki67-labeled cells (data not shown). Thus, the decrease in viable cell

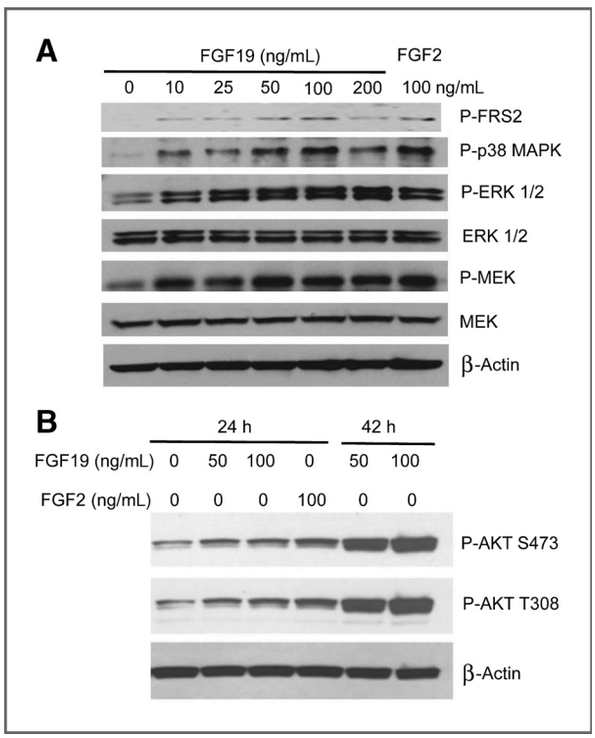

Figure 3. FGF19 activates MAP kinase and AKT pathways in prostate cancer cells. A, DU145 cells were serum starved for 24 hours and stimulated with the indicated concentration of FGF19 or FGF2 for 15 minutes. Cell lysates were prepared and Western blot analysis was conducted as described in Materials and Methods to assess activation of MAP kinase signaling. B, LNCaP cells were serum starved for 24 hours and then treated with the indicated concentration of FGF19 or FGF2 for either 24 or 42 hours. Cell lysates were prepared and Western blot analysis was conducted as described in Materials and Methods to assess the activation of AKT.

number was in large part due to a small, but significant, decrease in cell viability.

We then established stable cell lines in PC3 cells using the 2 shRNAs and analyzed the cell lines for FGF19 protein expression, proliferation, and invasion (Fig. 4C). FGF19 protein, as determined by ELISA, was decreased by approximately 50% for both shRNAs cell lines. Invasion was decreased 60% to 77%, whereas proliferation was decreased by 29% to 37%. Soft agar colony formation was decreased 40% to 43% (data not shown). Thus knockdown of autocrine FGF19 has significant effects on multiple cellular phenotypes related to transformation. Most striking is the impact on invasion, and our findings indicate that a significant fraction of cancer invasion in these 2 cell lines can be attributed to autocrine FGF19 expression.

We then carried out a subcutaneous xenograft experiment with one of the stable shFGF19 PC3 cells lines and vector controls. FGF19 knockdown resulted in a marked inhibition of tumor growth with minimal growth of tumor between days 13 and 32 after inoculation (Fig. 4D). Final tumor weight was 325 $\pm$ 6 mg ($n = 14$) in controls versus 73 $\pm$ 1 mg ($n = 18$) in FGF19sh1 cells (mean $\pm$ SEM, $P = 2.5 \times 10^{-5}$, t test). These studies confirm the important role of autocrine FGF19 in prostate cancer growth *in vivo*.

Expression of FGF19 in human prostate and prostate cancer tissues

To determine if FGF19 is expressed in prostate cancer, we measured FGF19 mRNA levels by qRT-PCR in using RNAs from 63 benign tissues and 73 prostate cancers. As shown in Fig. 5A, FGF19 mRNA was upregulated 3.8-fold in the cancer tissues ($P = 0.025$, t test). To confirm that FGF19 is expressed in prostate and/or prostate cancer tissues at the protein level, we carried out IHC with an anti-FGF19 antibody using a small tissue microarray containing 29 benign and 15 cancer tissues. Staining was graded as 0 to 3+ (negative, weak, moderate, and strong) in benign and neoplastic epithelium and stroma. Approximately 60% of cancer samples showed moderate staining in cancer cells. Stromal staining was also observed, predominantly in spindle-shaped cells, probably fibroblastic or myofibroblastic cells. An example of staining in a primary prostate cancer is shown in Fig. 5B. The mean staining in cancer epithelium was significantly higher in cancer than in benign epithelium (1.47 ± 0.13 versus 1.13 ± 0.07 mean $\pm$ SEM; $P = 0.02$, Mann–Whitney). We have also stained a small tissue microarray containing 17 metastatic prostate cancers. Interestingly, we found a highly dichotomous staining pattern. Eight of 17 metastatic cancers stained for FGF19 expression and 7 of 8 had strong staining and 1 moderate staining. Examples of this strong staining are shown in Fig. 5B. The other 9 cases were negative (Fig. 5B, bottom right). Thus about half of metastatic prostate cancer lesions express FGF19, almost all of which showed strong expression. Negative control with no primary antibody was completely negative in all cases. Overall, approximately half of all primary and metastatic prostate cancer express FGF19 protein.

Expression of Klotho coreceptors in human prostate and prostate cancer

We then examined laser-captured benign and cancer epithelium and stroma for expression of KL mRNA. All 3 normal epithelia and all 14 normal stroma tissues expressed KL. Somewhat surprisingly only 2 of 7 cancer epithelia expressed KL, whereas all 7 cancer stroma samples expressed KL. The RT-PCR for epithelial samples is shown in Fig. 6A. Examination of the Oncomine data bases reveals that KL is significantly higher in prostate cancer (as well as in renal cell carcinoma) compared with other cancers (t test $P = 4 \times 10^{-45}$; top Fig. 6B). Of note, KL is also significantly higher in normal prostate ($P = 2 \times 10^{-9}$, bottom Fig. 6B) and kidney compared with other normal tissues.

Analysis of KLB expression using the laser-captured samples described above showed no expression in normal epithelium, whereas expression was seen in 4 of 14 normal stromal samples. Two of 7 cancer epithelial samples and 4 of 7 cancer stroma samples expressed KLB. The data from the epithelial samples is shown in Fig. 6A. Of note, one cancer sample expressed both KL and KLB and overall 3 of 7 cancer epithelia express one or both Klotho coreceptors. Examination of the Oncomine database shows that KLB is significantly upregulated in prostate cancer versus normal prostate in multiple microarray datasets, including the Luo, Varambally, Varanaja, and Lapointe datasets (Fig. 6C, $P < 0.05$ for each dataset).

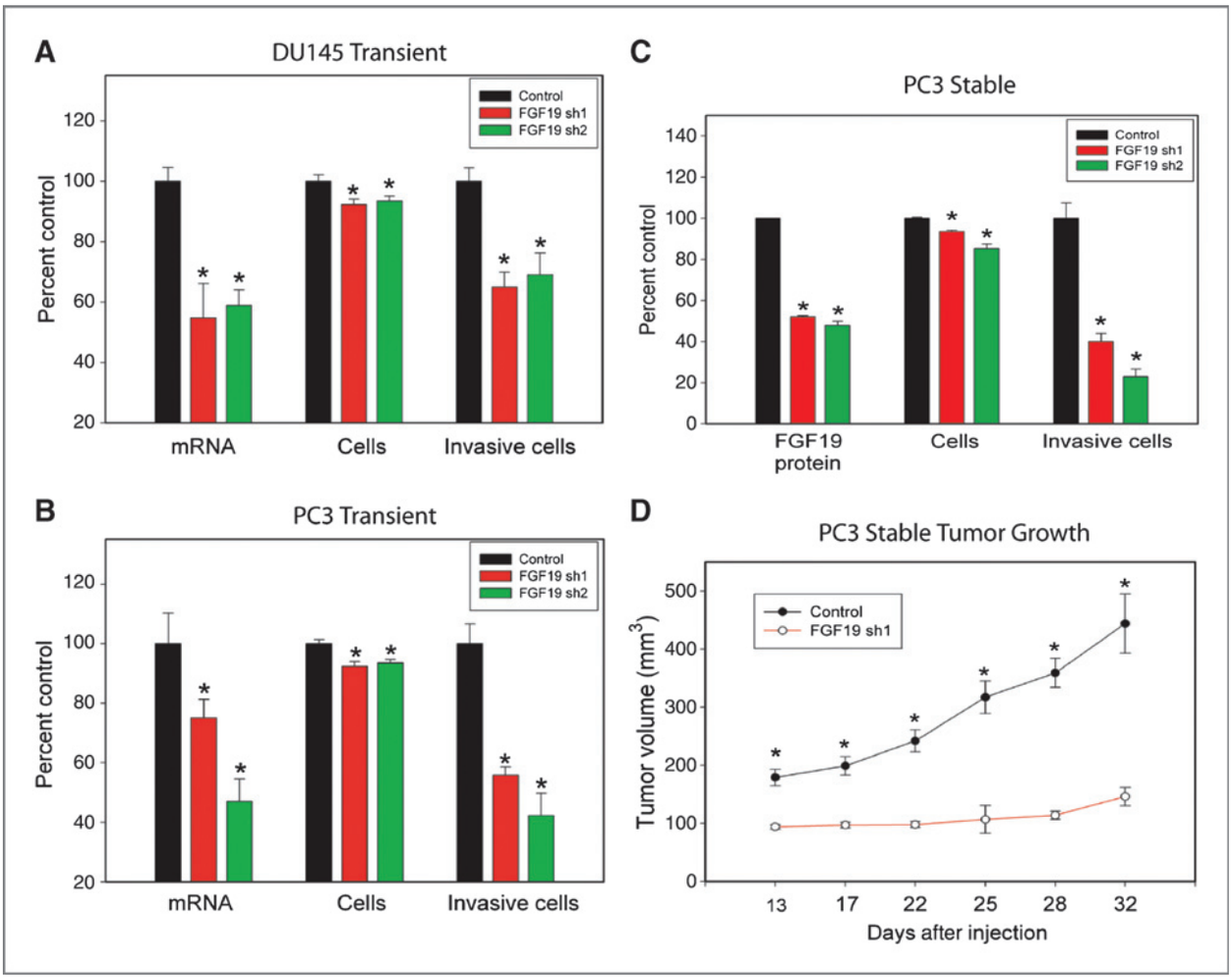

Figure 4. Biologic effects of FGF19 knockdown on prostate cancer cells. A and B, FGF19 was transiently knocked down using 2 different shRNAs and mRNA levels evaluated by qRT-PCR. Proliferation and invasion were evaluated on parallel plates as described in Materials and Methods. A, DU145 cells; B, PC3 cells. C, FGF19 was stably knocked down using 2 different shRNAs. Protein expression was determined using an FGF19 ELISA. Proliferation and invasion were evaluated on parallel plates as described in Materials and Methods. For A–C, experimental data are expressed relative to vector control cells (100%). The mean ± SD is shown. D, PC3 cells with knockdown of FGF19 (FGF19 sh1, $n = 18$) or vector controls ($n = 14$) were inoculated subcutaneously on day 1. Calculated tumor volume is shown at intervals from day 13 to day 32. Mean ± SEM is shown. Statistically significant differences from controls are indicated by asterisks for all experiments.

Immunohistochemical staining with anti-KL antibody showed variable expression of KL in normal and cancer epithelium. As shown in Fig. 7A, there is robust expression of KL in the tubules of the kidney, which is a well-known site of KL expression by IHC, and negative control showed no staining (not shown). Examination of a small tissue microarray of primary prostate cancer tissues revealed a dichotomous staining pattern. In 11 of 22 cases, there was strong staining of prostate cancer cells (Figs. 7B and C), whereas in 10 cases there was no staining or focal weak staining (not shown). One case had moderate staining. Negative control slides showed no staining. Normal epithelium showed weak staining in 8 of 16 cases with moderate staining in 6 of 16 cases (Fig. 7D) and no staining in 2 cases. Staining was variable both within luminal and basal cells. Variable stromal staining was also seen in both cancer and normal stroma in spindle-shaped cells and in endothelium. Thus KL protein is expressed in about one half of primary prostate cancer epithelium. Using a small tissue microarray of metastatic prostate cancer, we found that 16 of 20 cases had strong staining for KL and 2 had moderate staining, Thus 90% of metastatic prostate cancer lesions express KL at moderate or high levels, consistent with the finding that all prostate cancer cell lines (all derived from metastatic lesions) express KL.

Discussion

We have established for the first time that FGF19 plays a role in human prostate cancer. FGF19 is expressed in an autocrine manner at increased levels compared with benign prostatic epithelial cells in 3 of 4 prostate cancer cell lines and by immunohistochemistry in approximately half primary and metastatic prostate cancers. Suppression of FGF19 expression

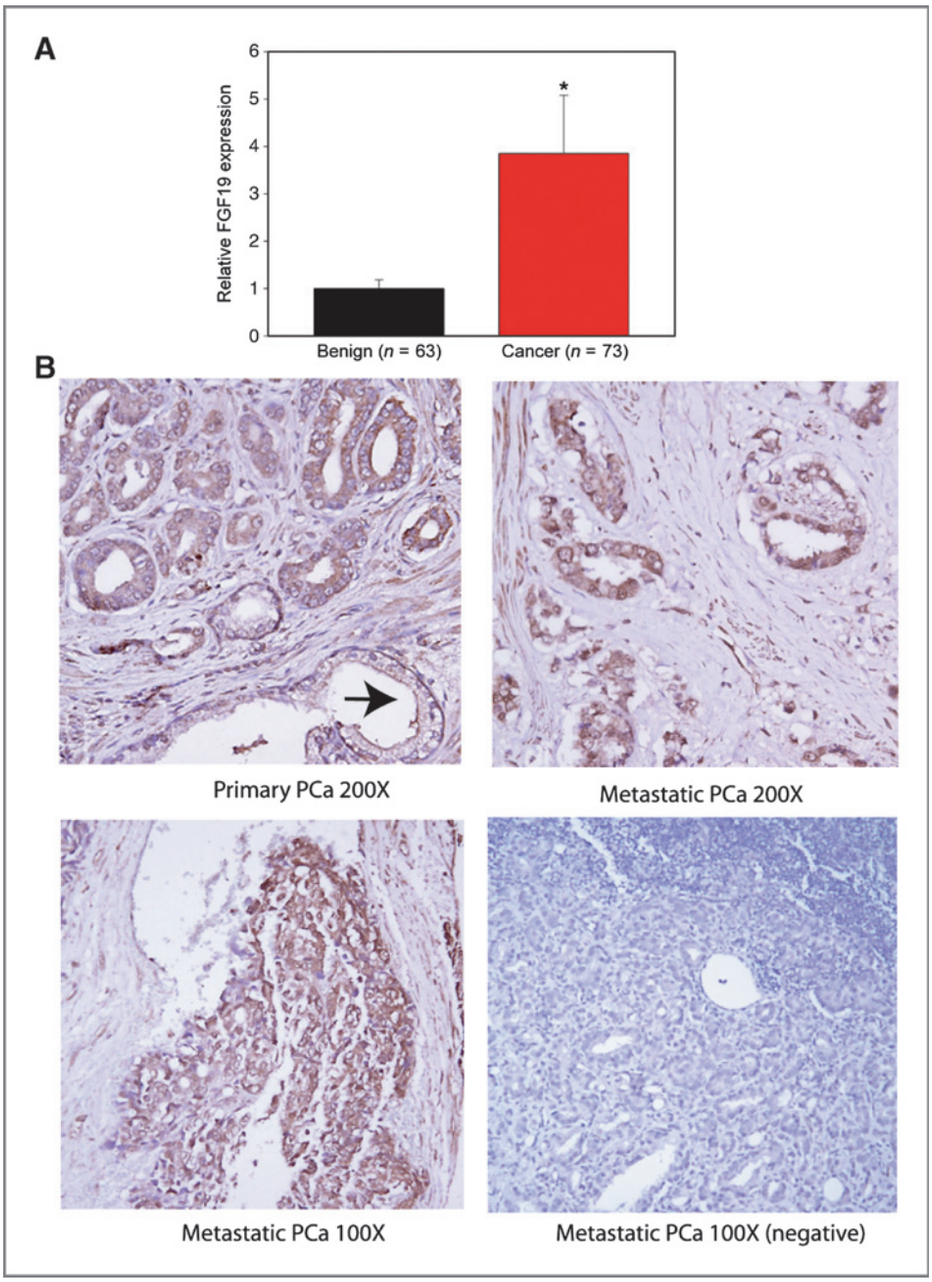

Figure 5. FGF19 is expressed in human prostate cancer tissues. A, qRT-PCR for FGF19 mRNA expression was conducted on 63 benign and 73 primary prostate cancer samples. Relative expression after normalization to HPRT is shown (mean ± SEM). The difference in FGF19 expression between benign and cancer samples was statistically significant ($P = 0.025$, *t* test). B, immunohistochemistry was conducted as described in Materials and Methods. Top left, medium power view (×200) of primary prostate cancer (PCa). Arrow shows normal epithelial cells. Top right (×200) and bottom left (×100), metastatic prostate cancer lesions with strong FGF19 expression. Bottom right, metastatic lesion with no FGF19 expression on same tissue microarray (×100).

by transient or stable transfection of FGF19 targeting shRNAs significantly inhibits prostate cancer cell invasion, colony formation, and proliferation *in vitro* and markedly inhibits tumor growth *in vivo*. Thus FGF19 can act as an autocrine factor to promote prostate cancer progression. Additional orthotopic studies in LNCaP cells (which do not express FGF19) with inducible expression of FGF19 would help clarify if FGF19 expression is sufficient to induce increased growth and/or metastasis in early- and/or later-stage tumors. Our IHC studies show that FGF19 is expressed in the stroma of a subset of primary prostate cancers, as seen in our prior laser capture microdissected prostate cancer stroma expression microarray data (22), and consistent with a paracrine mechanism of action in some cases. Our data also suggests that FGF19 can act as an endocrine factor to promote prostate cancer initiation and progression. The normal fasting FGF19 serum concentration is 0.19 ng/mL (range 0.05–0.59 ng/mL) and this doubles after meals in response to absorption of bile acids by the intestine, so average concentrations are in the range of 0.2 to 0.4 ng/mL throughout the course of the day. We see statistically significant effects on prostate cancer proliferation and adhesion *in vitro* at these levels of FGF19. The constant presence of FGF19 over decades may thus promote prostate cancer initiation and/or progression in an endocrine manner *in vivo*. Thus

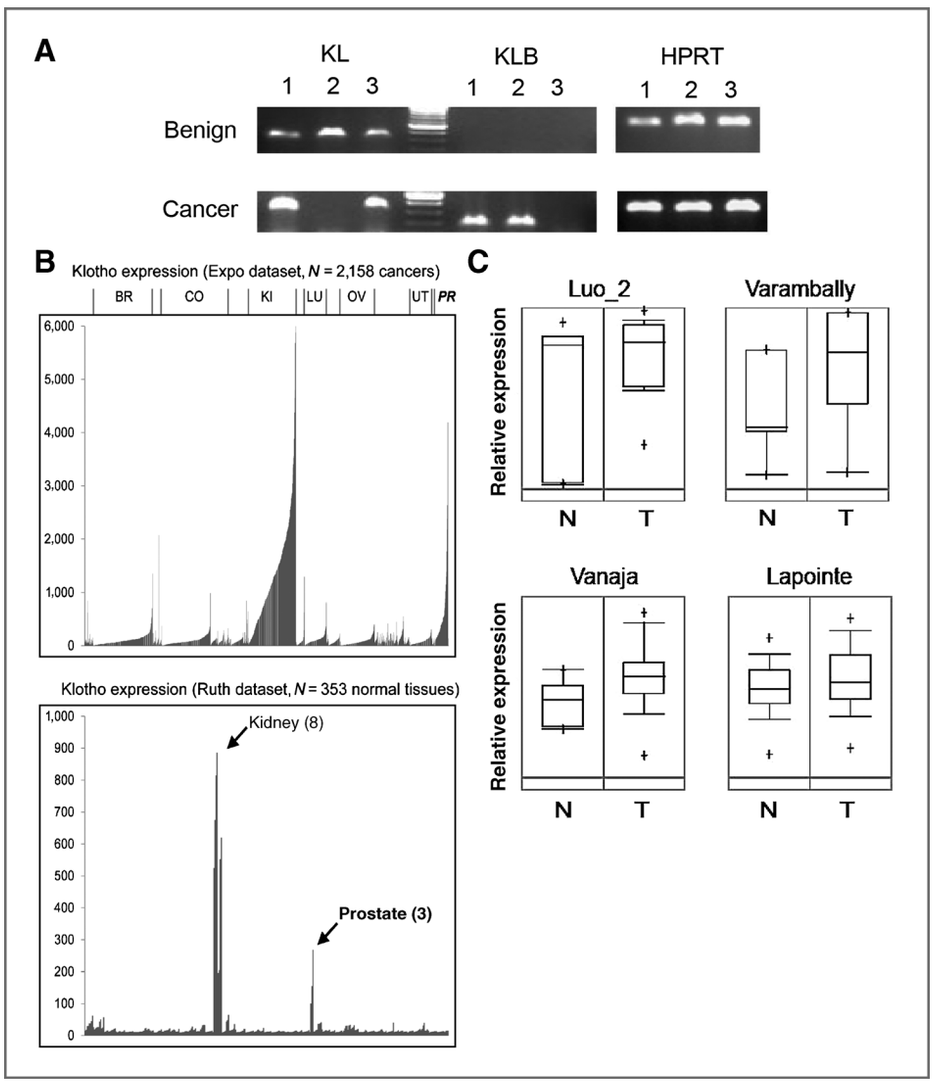

Figure 6. Expression of Klotho coreceptor mRNAs in human prostate and prostate cancer tissues. A, RT-PCR for KL and KLB mRNA in a laser-captured benign and cancer epithelium. HPRT is a reverse transcription control. B, KL mRNA levels across multiple tissue types (including prostate) for both cancer (top) and normal (bottom) tissues. Top, BR, breast; CO, colon; KI, kidney; LU, lung; OV, ovarian; UT, uterine; PR, prostate C. Relative expression of KLB in normal/benign prostate tissue (N) versus prostate tumors (T), for 4 independent profiling datasets (surveyed using Oncomine).

FGF19 can act as an autocrine, paracrine, and endocrine growth factor in prostate cancer. Additional studies will be needed to clarify the relative importance of these modes of action but it is likely to be variable between different tumors depending on the levels of autocrine and/or paracrine FGF19 expression.

To respond to low concentrations of FGF19, a Klotho coreceptor must be present in the cell as well as FGFR(s). The FGF19 coreceptor KL is expressed in most benign prostate epithelial tissue samples. In addition, it is expressed in immortalized normal prostatic epithelial cells. Interestingly, analysis of expression microarray data from Oncomine indicates that normal kidney and prostate have high levels of KL compared with other tissues. In kidney, KL is known to be expressed as the FGF23 coreceptor and plays a key role in phosphate and vitamin D metabolism (7). This data implies that KL may be playing a role in the biology of normal prostate epithelium. It is of interest that the PNT1a normal epithelial cell line is not as sensitive to FGF19-induced proliferation as the prostate cancer cell lines, implying that FGF19 may not be supporting normal epithelial growth. Furthermore, this suggests that additional genetic or epigenetic changes have occurred in prostate cancer cell lines that enhance the proliferative response to FGF19. KL is expressed in all the prostate cancer cell lines and in 2 of 7 laser-captured primary prostate cancer cell samples and in half of prostate cancers by IHC. It is unclear why the KL gene expression is present in only a subset of primary prostate cancer samples despite its expression in most benign samples. However, KL is expressed in 90% of metastatic lesions by IHC, suggesting that cells expressing KL may be more aggressive. It should be noted that both FGFR1 and FGFR4 are widely expressed in prostate cancer. In addition, KL is also present in cancer and benign stroma, including spindle-shaped cells and endothelial cells. It has been previously reported that HUVEC cells express KL (30). Renal cell cancers as well as prostate cancer both express significantly higher levels of KL than other cancers, suggesting that expression of KL is not universal in cancers and may reflect differences in the underlying biology of these tumors compared with other cancers.

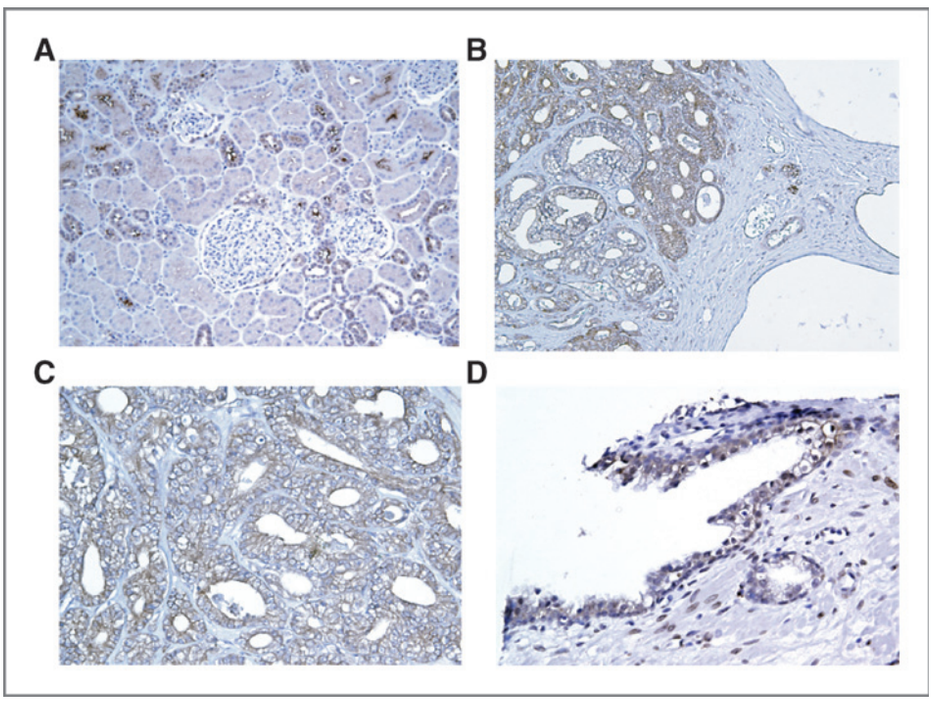

Figure 7. Expression of Klotho protein by immunohistochemistry. Immunohistochemistry was conducted as described in Materials and Methods. A, kidney (positive control; ×100). B, prostate cancer (×100); Cystic atrophy is present on the left. C, prostate cancer (×200). Note membranous staining pattern. D, normal epithelium with moderate staining (×200).

Previous reports indicate that KL can bind FGF19 and can activate ERK signaling in HEK293 cells transfected with KL and treated with FGF19 (10). Our finding that FGF19 can stimulate biologic activities in LNCaP cells, which express KL but not KLB, at concentrations as low as 0.25 ng/mL confirms that KL can act as a coreceptor for FGF19 in this cellular context as well. For comparison, in the absence of Klotho coreceptors 1,000 ng/mL of FGF19 is required to activate FGFR-4 (31). Thus, prostate cancer cells often express KL and thus can respond to FGF19 and potentially to FGF23, which also uses KL as a coreceptor.

Our data indicate that a subset of primary prostate cancers express KLB, which is not present in benign prostatic epithelium. This is consistent with our finding that 2 of 4 prostate cancer cell lines, but not a normal epithelial cell line, expresses KLB. Presumably, this expression reflects a selective process allowing for increased response to FGF19, and potentially to other endocrine FGFs, but further studies are needed to clarify this point. KLB is also variably expressed in cancer and normal stroma. The type of cells expressing KLB in stroma and the reason for the observed variability is unclear. Analysis of multiple Oncomine databases reveals that overall prostate cancer expresses higher levels of KLB than normal prostate. This probably reflects increased expression in malignant epithelium but it could also reflect increased stromal expression. Further studies are needed to clarify this point. Interestingly, we noted both in primary prostate cancer cells and cell lines that KL and KLB can be coexpressed, indicating that their functions are probably nonredundant in prostate cancer.

To activate signaling endocrine, FGFs require Klotho coreceptors. FGF23 requires KL (3), FGF21 requires KLB (3), and FGF19 can use either KL or KLB as described above. The presence of at least one Klotho coreceptor in all prostate cancer cell lines indicates that other endocrine FGFs in serum in addition to FGF19 are potential growth factors for prostate cancer. Endocrine FGFs are present at serum in healthy adults [approximate means: FGF19: 300 ng/L (28); FGF21: 200 ng/L (32); and FGF23: 30 ng/L (33)]. While these levels are relatively low compared with levels of classical FGFs used in tissue culture, given that endocrine FGFs have actions as hormones in serum, it is highly likely that they are capable of activating signaling in cells expressing the relevant coreceptors when present at these levels. Furthermore, endocrine FGFs are elevated in disease states, some of which have been linked to prostate cancer risk and/or aggressiveness. For example, mean serum levels of FGF23 in patients with renal failure are elevated 20- to 30-fold (33) and there are also more modest increases in FGF19 (34). Patients with less severe renal dysfunction also have elevated FGF23 (35). Of note, higher serum calcium, which is associated with higher FGF23 (33) is significantly associated with the incidence of fatal prostate cancer (36–37). Similarly, FGF21 has been shown to be increased in obesity (38), which is linked to fatal prostate cancer (39). Finally, FGF23 can potentially act as a paracrine factor in bone, the primary metastatic site for prostate cancer, since it is produced predominantly in osteoblasts and osteocytes (40). Further studies are needed to determine the role of FGF19 and other endocrine FGFs in prostate cancer progression and initiation.

Aberrant FGF signaling can promote tumor development by directly driving cancer cell proliferation, invasion and survival, and by supporting tumor angiogenesis (15, 41). These observations make FGF signaling networks increasingly attractive as targets for therapeutic intervention in cancer. Although targeting FGF signaling as a cancer therapeutic strategy has lagged

behind that of other receptor tyrosine kinases, there is now substantial evidence for the importance of FGF signaling in the pathogenesis of diverse tumor types, and clinical reagents that specifically target the FGFs and FGFRs are being developed (41). We have recently shown that inhibition of FGFR kinase activity using a small molecule inhibitor markedly decreases prostate cancer tumor progression *in vivo* (42). The finding that FGF19 and perhaps other endocrine FGFs can promote biologic activities in prostate cancer relevant to tumor progression gives further impetus to these efforts in prostate cancer, particularly anti-FGF19-targeted therapies.

Disclosure of Potential Conflicts of Interest

No potential conflicts of interest were disclosed.

Authors' Contributions

Conception and design: S. Feng, M.M. Ittmann
Development of methodology: S. Feng, O. Dakhova, M.M. Ittmann
Acquisition of data (provided animals, acquired and managed patients, provided facilities, etc.): S. Feng, O. Dakhova, M.M. Ittmann
Analysis and interpretation of data (e.g., statistical analysis, biostatistics, computational analysis): S. Feng, C.J. Creighton, M.M. Ittmann
Writing, review, and/or revision of the manuscript: S. Feng, M.M. Ittmann
Administrative, technical, or material support (i.e., reporting or organizing data, constructing databases): M.M. Ittmann
Study supervision: M.M. Ittmann

Acknowledgments

The assistance of Billie Smith with immunohistochemistry and Patricia Castro with tissue RNA extraction is gratefully acknowledged.

Grant Support

This work was supported by grants from the Department of Veterans Affairs Merit Review program (MI), the National Cancer Institute to the Dan L. Duncan Cancer (P30 CA125123), and by the use of the facilities of the Michael E. DeBakey VAMC.

The costs of publication of this article were defrayed in part by the payment of page charges. This article must therefore be hereby marked *advertisement* in accordance with 18 U.S.C. Section 1734 solely to indicate this fact.

Received October 31, 2012; revised December 28, 2012; accepted January 26, 2013; published OnlineFirst February 25, 2013.

References

1. Itoh N, Ornitz DM. Fibroblast growth factors: from molecular evolution to roles in development, metabolism and disease. J Biochem 2011;149:121–30.
2. Harmer NJ, Pellegrini L, Chirgadze D, Fernandez-Recio J, Blundell TL. The crystal structure of fibroblast growth factor (FGF) 19 reveals novel features of the FGF family and offers a structural basis for its unusual receptor affinity. Biochemistry 2004;43:629–40.
3. Kurosu H, Kuro OM. The Klotho gene family as a regulator of endocrine fibroblast growth factors. Mol Cell Endocrinol 2009;299:72–8.
4. Fu L, John LM, Adams SH, Yu XX, Tomlinson E, Renz M, et al. Fibroblast growth factor 19 increases metabolic rate and reverses dietary and leptin-deficient diabetes. Endocrinology 2004;145: 2594–603.
5. Choi M, Moschetta A, Bookout AL, Peng L, Umetani M, Holmstrom SR, et al. Identification of a hormonal basis for gallbladder filling. Nat Med 2006;12:1253–5.
6. Kharitonenkov A, Shiyanova TL, Koester A, Ford AM, Micanovic R, Galbreath EJ, et al. FGF-21 as a novel metabolic regulator. J Clin Invest 2005;115:1627–35.
7. Hori M, Shimizu Y, Fukumoto S. Minireview: fibroblast growth factor 23 in phosphate homeostasis and bone metabolism. Endocrinology 2011;152:4–10.
8. Xie MH, Holcomb I, Deuel B, Dowd P, Huang A, Vagts A, et al. FGF-19, a novel fibroblast growth factor with unique specificity for FGFR4. Cytokine 1999;11:729–35.
9. Kurosu H, Choi M, Ogawa Y, Dickson AS, Goetz R, Eliseenkova AV, et al. Tissue-specific expression of betaKlotho and fibroblast growth factor (FGF) receptor isoforms determines metabolic activity of FGF19 and FGF21. J Biol Chem 2007;282:26687–95.
10. Wu X, Ge H, Gupte J, Weiszmann J, Shimamoto G, Stevens J, et al. Co-receptor requirements for fibroblast growth factor-19 signaling. J Biol Chem 2007;282:29069–72.
11. Wu X, Lemon B, Li X, Gupte J, Weiszmann J, Stevens J, et al. C-terminal tail of FGF19 determines its specificity toward Klotho co-receptors. J Biol Chem 2008;283:33304–9.
12. Nicholes K, Guillet S, Tomlinson E, Hillan K, Wright B, Frantz GD, et al. A mouse model of hepatocellular carcinoma: ectopic expression of fibroblast growth factor 19 in skeletal muscle of transgenic mice. Am J Pathol 2002;160:2295–307.
13. Desnoyers LR, Pai R, Ferrando RE, Hotzel K, Le T, Ross J, et al. Targeting FGF19 inhibits tumor growth in colon cancer xenograft and FGF19 transgenic hepatocellular carcinoma models. Oncogene 2008;27:85–97.
14. Pai R, Dunlap D, Qing J, Mohtashemi I, Hotzel K, French DM. Inhibition of fibroblast growth factor 19 reduces tumor growth by modulating beta-catenin signaling. Cancer Res 2008;68:5086–95.
15. Kwabi-Addo B, Ozen M, Ittmann M. The role of fibroblast growth factors and their receptors in prostate cancer. Endocr Relat Cancer 2004;11:709–24.
16. Giri D, Ropiquet F, Ittmann M. Alterations in expression of basic fibroblast growth factor (FGF) 2 and its receptor FGFR-1 in human prostate cancer. Clin Cancer Res 1999;5:1063–71.
17. Acevedo VD, Gangula RD, Freeman KW, Li R, Zhang Y, Wang F, et al. Inducible FGFR-1 activation leads to irreversible prostate adenocarcinoma and an epithelial-to-mesenchymal transition. Cancer Cell 2007;12:559–71.
18. Wang J, Stockton DW, Ittmann M. The fibroblast growth factor receptor-4 Arg388 allele is associated with prostate cancer initiation and progression. Clin Cancer Res 2004;10:6169–78.
19. Gowardhan B, Douglas DA, Mathers ME, McKie AB, McCracken SR, Robson CN, et al. Evaluation of the fibroblast growth factor system as a potential target for therapy in human prostate cancer. Br J Cancer 2005;92:320–7.
20. Sahadevan K, Darby S, Leung HY, Mathers ME, Robson CN, Gnanapragasam VJ. Selective over-expression of fibroblast growth factor receptors 1 and 4 in clinical prostate cancer. J Pathol 2007;213:82–90.
21. Murphy T, Darby S, Mathers ME, Gnanapragasam VJ. Evidence for distinct alterations in the FGF axis in prostate cancer progression to an aggressive clinical phenotype. J Pathol 2010;220:452–60.
22. Dakhova O, Ozen M, Creighton CJ, Li R, Ayala G, Rowley D, et al. Global gene expression analysis of reactive stroma in prostate cancer. Clin Cancer Res 2009;15:3979–89.
23. Yu W, Feng S, Dakhova O, Creighton CJ, Cai Y, Wang J, et al. FGFR-4 Arg(3) enhances prostate cancer progression via extracellular signal-related kinase and serum response factor signaling. Clin Cancer Res 2011;17:4355–66.
24. Wang J, Cai Y, Shao LJ, Siddiqui J, Palanisamy N, Li R, et al. Activation of NF-{kappa}B by TMPRSS2/ERG Fusion Isoforms through Toll-Like Receptor-4. Cancer Res 2011;71:1325–33.
25. Roth RB, Hevezi P, Lee J, Willhite D, Lechner SM, Foster AC, et al. Gene expression analyses reveal molecular relationships among 20 regions of the human CNS. Neurogenetics 2006;7:67–80.
26. Rhodes DR, Kalyana-Sundaram S, Mahavisno V, Varambally R, Yu J, Briggs BB, et al. Oncomine 3.0: genes, pathways, and networks in a collection of 18,000 cancer gene expression profiles. Neoplasia 2007; 9:166–80.

27. Stejskal D, Karpisek M, Hanulova Z, Stejskal P. Fibroblast growth factor-19: development, analytical characterization and clinical evaluation of a new ELISA test. Scand J Clin Lab Invest 2008;68: 501–7.
28. Lundasen T, Galman C, Angelin B, Rudling M. Circulating intestinal fibroblast growth factor 19 has a pronounced diurnal variation and modulates hepatic bile acid synthesis in man. J Intern Med 2006;260:530–6.
29. Lafrenie RM, Buckner CA, Bewick MA. Cell adhesion and cancer: is there a potential for therapeutic intervention? Expert Opin Ther Targets 2007;11:727–31.
30. Liu F, Wu S, Ren H, Gu J. Klotho suppresses RIG-I-mediated senescence-associated inflammation. Nat Cell Biol 2011;13:254–62.
31. Wu X, Ge H, Lemon B, Weiszmann J, Gupte J, Hawkins N, et al. Selective activation of FGFR4 by an FGF19 variant does not improve glucose metabolism in *ob/ob* mice. Proc Natl Acad Sci U S A 2009;106:14379–84.
32. Lin Z, Wu Z, Yin X, Liu Y, Yan X, Lin S, et al. Serum levels of FGF-21 are increased in coronary heart disease patients and are independently associated with adverse lipid profile. PLoS One 2010;5:e15534.
33. Kazama JJ, Sato F, Omori K, Hama H, Yamamoto S, Maruyama H, et al. Pretreatment serum FGF-23 levels predict the efficacy of calcitriol therapy in dialysis patients. Kidney Int 2005;67:1120–5.
34. Reiche M, Bachmann A, Lossner U, Bluher M, Stumvoll M, Fasshauer M. Fibroblast growth factor 19 serum levels: relation to renal function and metabolic parameters. Horm Metab Res 2010;42: 178–81.
35. Oliveira RB, Cancela AL, Graciolli FG, Dos Reis LM, Draibe SA, Cuppari L, et al. Early control of PTH and FGF23 in normophosphatemic CKD patients: a new target in CKD–MBD therapy? Clin J Am Soc Nephrol 2010;5:286–91.
36. Skinner HG, Schwartz GG. Serum calcium and incident and fatal prostate cancer in the National Health and Nutrition Examination Survey. Cancer Epidemiol Biomarkers Prev 2008;17:2302–5.
37. Skinner HG, Schwartz GG. A prospective study of total and ionized serum calcium and fatal prostate cancer. Cancer Epidemiol Biomarkers Prev 2009;18:575–8.
38. Zhang X, Yeung DC, Karpisek M, Stejskal D, Zhou ZG, Liu F, et al. Serum FGF21 levels are increased in obesity and are independently associated with the metabolic syndrome in humans. Diabetes 2008;57:1246–53.
39. Snowdon DA, Phillips RL, Choi W. Diet, obesity, and risk of fatal prostate cancer. Am J Epidemiol 1984;120:244–50.
40. Quarles LD. Skeletal secretion of FGF-23 regulates phosphate and vitamin D metabolism. Nat Rev Endocrinol 2012;8:276–86.
41. Turner N, Grose R. Fibroblast growth factor signalling: from development to cancer. Nat Rev Cancer 2010;10:116–29.
42. Feng S, Shao L, Yu W, Gavine P, Ittmann M. Targeting fibroblast growth factor receptor signaling inhibits prostate cancer progression. Clin Cancer Res 2012;18:3880–8.